

UC Davis

UC Davis Previously Published Works

Title

HiFi chromosome-scale diploid assemblies of the grape rootstocks 110R, Kober 5BB, and 101–14 Mgt

Permalink

<https://escholarship.org/uc/item/4xk0q8kt>

Journal

Scientific Data, 9(1)

ISSN

2052-4463

Authors

Minio, Andrea

Cochetel, Noé

Massonnet, Mélanie

et al.

Publication Date

2022

DOI

10.1038/s41597-022-01753-0

Copyright Information

This work is made available under the terms of a Creative Commons Attribution License, available at <https://creativecommons.org/licenses/by/4.0/>

Peer reviewed



OPEN

DATA DESCRIPTOR

HiFi chromosome-scale diploid assemblies of the grape rootstocks 110R, Kober 5BB, and 101–14 Mgt

Andrea Minio, Noé Cochetel[✉], Mélanie Massonnet[✉], Rosa Figueroa-Balderas & Dario Cantu[✉]

Cultivated grapevines are commonly grafted on closely related species to cope with specific biotic and abiotic stress conditions. The three North American *Vitis* species *V. riparia*, *V. rupestris*, and *V. berlandieri*, are the main species used for breeding grape rootstocks. Here, we report the diploid chromosome-scale assembly of three widely used rootstocks derived from these species: Richter 110 (110R), Kober 5BB, and 101–14 Millardet et de Grasset (Mgt). Draft genomes of the three hybrids were assembled using PacBio HiFi sequences at an average coverage of 53.1 X-fold. Using the tool suite HaploSync, we reconstructed the two sets of nineteen chromosome-scale pseudomolecules for each genome with an average haploid genome size of 494.5 Mbp. Residual haplotype switches were resolved using shared-haplotype information. These three reference genomes represent a valuable resource for studying the genetic basis of grape adaption to biotic and abiotic stresses, and designing trait-associated markers for rootstock breeding programs.

Background & Summary

Cultivated grapevines (*Vitis vinifera* ssp. *vinifera*) are usually grafted onto rootstocks derived from North American *Vitis* species (Fig. 1a). This practice was established during the 19th century in response to the near devastation of European vineyards by the grape root aphid phylloxera (*Daktulosphaira vitifoliae* Fitch)¹. Grape phylloxera was introduced into Europe in the 1850s through the movement of plant material from North America². Most North American *Vitis* species are resistant to phylloxera, likely as a result of co-evolution with the insect in their native environment. *Vitis riparia* and *Vitis rupestris* were the first wild grape species used as rootstock because they root easily from hardwood cuttings and have good grafting compatibility with the berry-producing scions³. However, these two species were not suitable for calcareous soils, which are common in Europe. *Vitis berlandieri*, another North American grape species, was then found to be resistant to phylloxera and lime-tolerant, although it poorly roots from dormant cuttings⁴. To introduce the lime-tolerance of *V. berlandieri* and improve its rootability, new rootstocks were bred crossing *V. berlandieri* with either *V. riparia* or *V. rupestris*. Today, commercialized rootstocks are mainly hybrids of these three grape species⁵. Among these, Richter 110 (110R; *V. berlandieri* x *V. rupestris*), Kober 5BB (*V. berlandieri* x *V. riparia*), and 101–14 Millardet et de Grasset (Mgt; *V. riparia* x *V. rupestris*) are the most commonly used worldwide (Fig. 1b). In addition to their resistance to phylloxera, grape rootstocks are chosen based on tolerance to biotic (e.g. nematodes) and abiotic stresses (e.g. drought), preference of soil physico-chemical properties, and the vigor level they confer to the scion⁶. For instance, 101–14 Mgt generally triggers the precocity of the vegetative growth despite a moderate vigor, whereas 110R and Kober 5BB confer high vigor and delay plant maturity⁷. 110R is known for its drought tolerance and excess soil moisture has negative impacts on its development⁶. In contrast, 101–14 Mgt and Kober 5BB are not considered drought-tolerant and grow well in moist soils⁶. The three rootstocks also have different levels of tolerance to nematodes depending on the nematode species^{6,8}.

In addition to their commercial importance, rootstocks are valuable to study the genetic bases of grape adaptation to biotic and abiotic stresses⁹. However, to date only two genomes of *V. riparia* have been published^{10,11} and no reference genome is available for any of the commonly used rootstocks. This article describes the chromosome-scale assemblies of 110R, Kober 5BB, and 101–14 Mgt. Genomes were sequenced using highly accurate long-read sequencing (HiFi, Pacific Biosciences) and assembled with Hifiasm¹². Each diploid draft genome was then scaffolded into two sets of pseudomolecules using the tool suite HaploSync¹³, and haplotypes

Department of Viticulture and Enology, University of California Davis, Davis, CA, 95616, USA. ✉e-mail: dacantu@ucdavis.edu

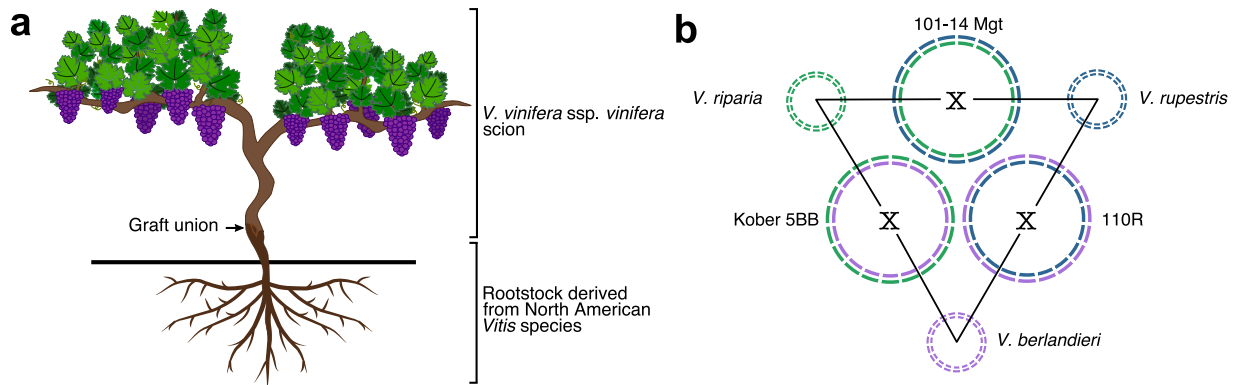


Fig. 1 Description of the three grape rootstocks 101–14 Mgt, 110R, and Kober 5BB. **(a)** Wine grapevine scion (*Vitis vinifera* spp. *vinifera*) grafted onto a rootstock from another *Vitis* species. **(b)** Schematic representation of haplotype composition of 101–14 Mgt, 110R, and Kober 5BB. Each pair of rootstocks shares a set of chromosomes from the same parental *Vitis* species. Shared haplotypes are represented with the same color.

were assigned to each *Vitis* parent based on sequence similarity between the haplotypes derived from the same species. These genomes represent an important resource for investigating the genetic basis of resistance to environmental factors and designing markers to accelerate rootstock breeding programs.

Methods

Library preparation and sequencing. Young leaves (1–2 cm-wide) were collected from 110R (FPS 01), Kober 5BB (FPS 06), and 101–14 Mgt (FPS 01) at Foundation Plant Services (University of California Davis, Davis, CA) and immediately frozen and ground to powder in liquid nitrogen. High molecular weight genomic DNA was extracted from 1 g of ground leaf tissue as described in Chin *et al.*¹⁴, and 12 µg of high molecular weight gDNA was sheared to a size distribution between 15 and 20 kbp using the Megaruptor[®] 2 (Diagenode, Denville, NJ, USA). For each accession, one HiFi sequencing library was prepared using the SMRTbell[®] Express Template Prep Kit 2.0 followed by immediate treatment with the Enzyme Clean Up Kit (Pacific Biosciences, Menlo Park, CA, USA). Libraries were size-selected using a BluePippin (Sage Sciences, Beverly, MA, USA) and HiFi SMRTbell[®] templates longer than 15 kbp were collected. Size-selected library fractions were cleaned using AMPure PB beads (Pacific Biosciences, Menlo Park, CA, USA). Concentration and final size distribution of the libraries were evaluated using a Qubit[™] 1X dsDNA HS Assay Kit (Thermo Fisher, Waltham, MA, USA) and Femto Pulse System (Agilent, Santa Clara, CA, USA), respectively. HiFi libraries of 110R and Kober 5BB were sequenced using a PacBio Sequel II system (Pacific Biosciences, CA, USA) at the DNA Technology Core Facility, University of California, Davis (Davis, CA, USA). For 101–14 Mgt, sequencing was performed by Corteva Agriscience (Johnston, IA, USA) as an award from Pacific Biosciences to Dr. Noé Cochetel. An average of 26.5 ± 3.8 Gbp sequences were generated for each genome, corresponding to 53.1 ± 7.7 X-fold coverage of a 500 Mbp haploid genome (Table 1).

Total RNA from *V. berlandieri* 9031, *V. rupestris* B38, and *V. riparia* HP-1 (PI588271) leaves was isolated using a Cetyltrimethyl Ammonium Bromide (CTAB)-based extraction protocol as described in Blanco-Ulate *et al.*¹⁵. RNA purity was evaluated with a Nanodrop 2000 spectrophotometer (Thermo Scientific, Hanover Park, IL, USA), and RNA integrity by electrophoresis and an Agilent 2100 Bioanalyzer (Agilent Technologies, CA, USA). RNA quantity was assessed with a Qubit 2.0 Fluorometer and a broad range RNA kit (Life Technologies, Carlsbad, CA, USA). Total RNA (300 ng, RNA Integrity Number >8.0) were used for library construction. Short-read cDNA libraries were prepared using the Illumina TruSeq RNA sample preparation kit v.2 (Illumina, CA, USA) following Illumina[™] low-throughput protocol. Libraries were evaluated for quantity and quality with the High Sensitivity chip and an Agilent 2100 Bioanalyzer (Agilent Technologies, CA, USA). One library per species was sequenced using an Illumina HiSeq 4000 sequencer with a 2x100bp protocol (DNA Technology Core Facility, University of California, Davis, CA, USA). Long-read cDNA SMRTbell libraries were prepared for *V. berlandieri* and *V. riparia*. First-strand synthesis and cDNA amplification were accomplished using the NEB Next Single Cell/Low Input cDNA Synthesis & Amplification Module (New England, Ipswich, MA, USA). The cDNAs were subsequently purified with ProNex magnetic beads (Promega, WI, USA) following the instructions in the Iso-Seq Express Template Preparation for Sequel and Sequel II Systems protocol (Pacific Biosciences, Menlo Park, CA, USA). ProNex magnetic beads (86 µL) were used to select amplified cDNA (≥ 2 kbp). At least 80 ng of the size-selected amplified cDNA were used to prepare the cDNA SMRTbell library. DNA damage repair and SMRTbell ligation was performed with SMRTbell Express Template Prep Kit 2.0 (Pacific Biosciences, Menlo Park, CA, USA) following the manufacturer's protocol. One SMRT cell was sequenced for each species on the PacBio Sequel I platform (DNA Technology Core Facility, University of California, Davis, CA, USA).

Genome assembly and pseudomolecule construction. HiFi reads were assembled using Hifiasm v.0.16.1-r374¹². Multiple combinations of several assembly parameters were tested. A total of 1,939 assemblies were generated. The least fragmented assembly of each genotype was selected. The selected draft assemblies

	101–14Mgt				110R				Kober 5BB											
Sequencing																				
Sequencing Depth (Gbp) X-Fold coverage*	26.3				30.5				22.8											
	53x				61x				46x											
Draft Assembly																				
Cumulative length (bp)	1,021,000,930				1,006,052,903				1,018,035,111											
Number of sequences	656				348				214											
Average sequence length (bp)	1,556,404				2,890,957				4,757,173											
Maximum sequence length (bp)	38,550,893				40,445,604				32,011,292											
N50 Length (bp)	14,459,101				13,727,353				14,854,816											
N50 Index	24				28				26											
	Count		%		Count		%		Count		%									
Complete BUSCOs (Total 2,326)	2,290		98.5%		2,295		98.7%		2,294		98.6%									
Complete BUSCOs Single	18		0.8%		27		1.2%		74		3.2%									
Complete BUSCOs Duplicated	2,272		97.7%		2,268		97.5%		2,220		95.4%									
Pseudomolecules																				
	Haplotype <i>V. riparia</i>		Haplotype <i>V. rupestris</i>		Unplaced		Haplotype <i>V. berlandieri</i>		Haplotype <i>V. rupestris</i>		Unplaced		Haplotype <i>V. berlandieri</i>		Haplotype <i>V. riparia</i>		Unplaced			
Cumulative length (bp)	492,356,428		492,600,706		36,133,067		495,178,401		491,477,282		19,903,444		505,179,188		489,908,332		23,334,789			
GC percentage	35.0%		34.8%		43.6%		34.6%		34.7%		47.0%		34.7%		35.0%		42.3%			
Number of sequences	19		19		527		19		19		215		19		19		92			
Average sequence length (bp)	25,913,496		25,926,352		68,564		26,062,021		25,867,225		92,574		26,588,378		25,784,649		253,639			
N50 Length (bp)	25,475,941		25,378,183		69,079		26,414,266		25,747,756		143,097		26,431,197		25,800,664		2,015,173			
N50 Index	9		9		116		9		9		29		9		9		5			
	Count		%		Count		%		Count		%		Count		%		Count		%	
Complete BUSCOs (Total 2,326)	2,284	98.2%	2,284	98.2%	9	0.4%	2,282	98.1%	2,276	97.9%	2	0.1%	2,286	98.3%	2,283	98.2%	37	1.6%		
Complete BUSCOs Single	2,240	96.3%	2,240	96.3%	9	0.4%	2,239	96.3%	2,230	95.9%	2	0.1%	2,239	96.3%	2,237	96.2%	34	1.5%		
Complete BUSCOs Duplicated	44	1.9%	44	1.9%	0	0.0%	43	1.8%	46	2.0%	0	0.0%	47	2.0%	46	2.0%	3	0.1%		
PN40024 unique genes (Total 28,243)	26,868	95.1%	26,802	94.9%	352	1.3%	26,854	95.1%	26,836	95.0%	402	1.4%	26,866	95.1%	26,791	94.9%	761	2.7%		
Annotated Genes	33,147		33,611		6,000		28,110		27,678		980		29,620		28,927		1,260			
Annotated Proteins	83,091		83,455		6,217		50,909		49,418		1,048		54,187		53,912		1,588			
Repeat content	50.4%		50.0%		53.9%		49.3%		49.6%		75.2%		49.9%		50.3%		75.0%			

Table 1. Genome assembly statistics of the three rootstocks. *based on 500Mbp genome size Summary statistics of the genome sequencing, draft genome assembly, chromosome-scale genome assembly, and gene annotation of 101–14 Mgt, 110R, and Kober 5BB rootstocks.

consisted of 406 ± 226 contigs with a $N50 = 14.3 \pm 0.6$ Mbp (Table 1). Compared to other grape genomes previously generated with PacBio CLR technology, the PacBio HiFi reads greatly improves the contiguity of the draft assembly (PacBio CLR 1.2 ± 0.3 Mbp, Fig. 2a). Gene space completeness was assessed using BUSCO V.5.1 with the Viridiplantae and Embryophyta ODB10 datasets¹⁶ and by mapping PN40024 (V1 annotation¹⁷) single-copy genes using GMAP v.2019-09-12 (alignments with at least 80% coverage and 80% identity were considered). For each rootstock, the draft genome assembly underwent quality control and scaffolding into a diploid set of chromosome-scale pseudomolecules using HaploSync¹³ and the *Vitis* consensus genetic map developed by Zou *et al.*¹⁸. One cycle of HaploFill was used for each genotype. The use of PacBio HiFi reads reduced significantly the fragmentation of the draft assembly compared to recently published grape genomes sequenced using PacBio CLR technology (Fig. 2b)^{13,14,19}. The lower fragmentation resulted in a 15 times smaller number of contigs necessary to scaffold a pseudomolecule (3.6 ± 2.0 HiFi contigs/pseudomolecule vs. 43.0 ± 20.6 CLR contigs/pseudomolecule) (Fig. 2b). Remarkably, in total across the three genomes, fifteen pseudomolecules were reconstructed from a single contig. Haplotype switches were identified based on sequence similarity of protein-coding sequences. Gene loci sequences of each rootstock were aligned against each others using minimap2 v.2.17-r941²⁰ and the

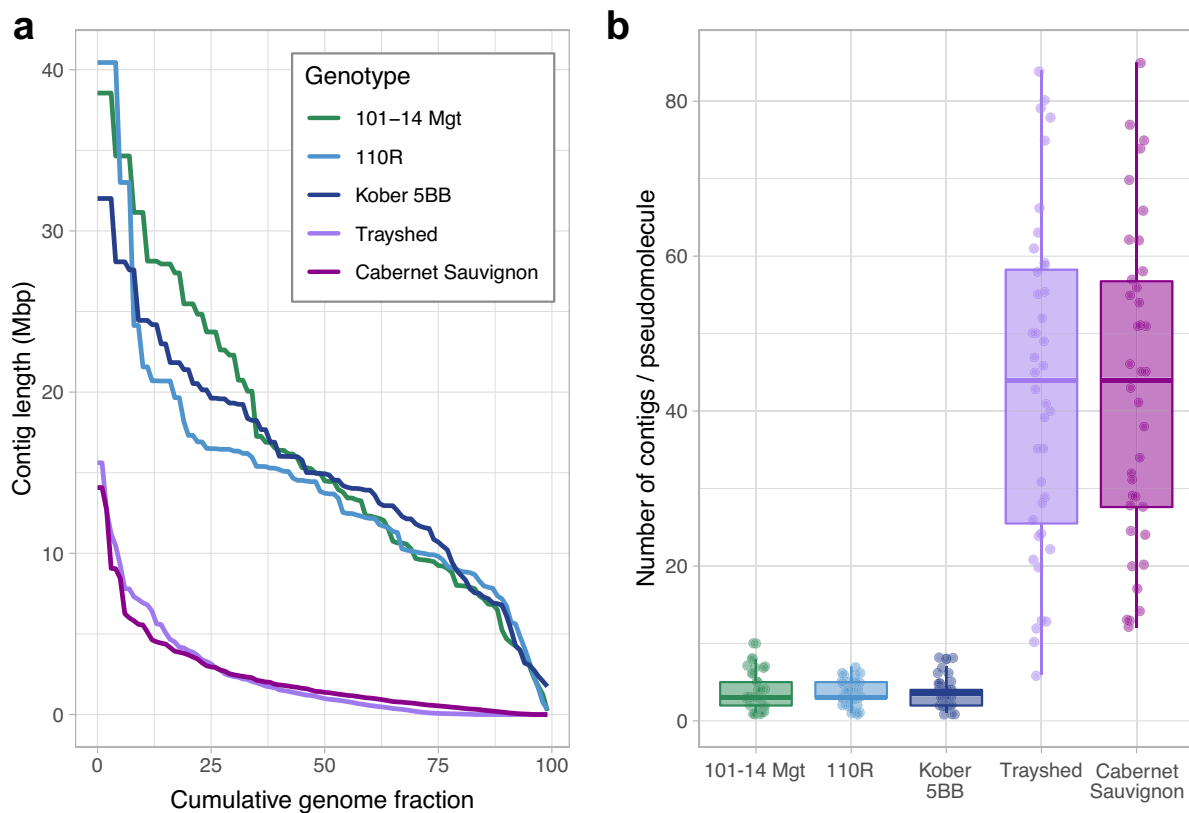


Fig. 2 PacBio HiFi sequencing technology substantially improves the contiguity of *Vitis* draft genome assembly. **(a)** Draft assembly fragmentation of 101–14 Mgt, 110R, Kober 5BB represented as distribution of contig NG(x) values. *Muscadidia rotundifolia* cv. Trayshed and *V. vinifera* cv. Cabernet Sauvignon, produced with CLR reads, were included as comparison. The NG(x) value is defined as the sequence length of the shortest contig necessary to achieve, cumulatively, a given fraction (x) of the expected diploid genome length (1 Gbp) when sequences are sorted from the longest to the shortest. Diploid assemblies produced with PacBio HiFi reads (101–14 Mgt, 110R, and Kober 5BB) resulted in a much more contiguous draft genome assembly compared to other grape genomes assembled with older long-read sequencing technologies despite a lower X-Fold coverage employed (PacBio Sequel CLR reads for Trayshed 140x X-Fold coverage,^{19,21} PacBio RSII CLR reads for Cabernet Sauvignon, 115X X-Fold coverage¹⁴). **(b)** Distribution of the number of contig scaffolded into complete pseudomolecules. The substantially lower fragmentation of the draft assemblies generated using PacBio HiFi reads (101–14 Mgt, 110R, and Kober 5BB) resulted on average in a 15x smaller number of contigs necessary to build a pseudomolecule.

parameter “-x map-hifi”. Alignments with the highest coverage and identity were used to assign common species parentage and to detect haplotype switches along pseudomolecules (Fig. 3a). After manual correction of the haplotype switches, a second cycle of HaploFill¹³ was performed using the pseudomolecules derived from the same *Vitis* species as alternative haplotypes to help closing gaps with draft sequences.

Gene prediction and repeat annotation. Gene structural annotations were predicted using the procedures described in https://github.com/andreaminio/AnnotationPipeline-EVM_based-DClab²¹. For each rootstock, Iso-Seq data from the corresponding parental species were concatenated with the *de novo* assembled transcripts from RNA-seq reads before generating the gene models. Iso-Seq libraries underwent extraction, demultiplexing and error correction using IsoSeq3 v.3.3.0 protocol (<https://github.com/PacificBiosciences/IsoSeq>). Low-quality and single isoforms dataset were further polished using LSC v2.0²². RNA-seq reads were quality-filtered and adapters were trimmed with Trimmomatic v.0.36 and the options “ILLUMINACLIP:2:30:10 LEADING:7 TRAILING:7 SLIDINGWINDOW:10:20 MINLEN:36”²³. High-quality RNA-seq reads from each *Vitis* species were assembled with three different protocols: (i) Trinity v.2.6.5²⁴ with the “*de novo*” protocol, (ii) Trinity v.2.6.5²⁴ using the “On-genome” protocol, (iii) Stringtie v.1.3.4d²⁵ using the reads found to align on the genome sequences with HISAT2 v.2.0.5 and the parameter “--very-sensitive”²⁶. Transcript sequences common to the three assembly methods were then pooled with the Iso-Seq reads. Sequence redundancy was reduced using CD-HIT v4.6²⁷ with the parameters “cd-hit-est -c 0.99 -g 0 -r 0 -s 0.70 -aS 0.99”. Non-redundant transcripts were processed with PASA v.2.3.3²⁸ to obtain the final training model sets. Combined with data from public databases, the derived transcript and protein evidences were aligned on the genome assembly using a multi-aligner pipeline including Exonerate v.2.2.0²⁹ and Pasa v.2.3.3²⁸. To produce the final set of consensus gene models with EvidenceModeler v.1.1.1³⁰, *ab initio* predictions were also generated using Augustus v.3.0.3³¹, BUSCO v.3.0.2³²,

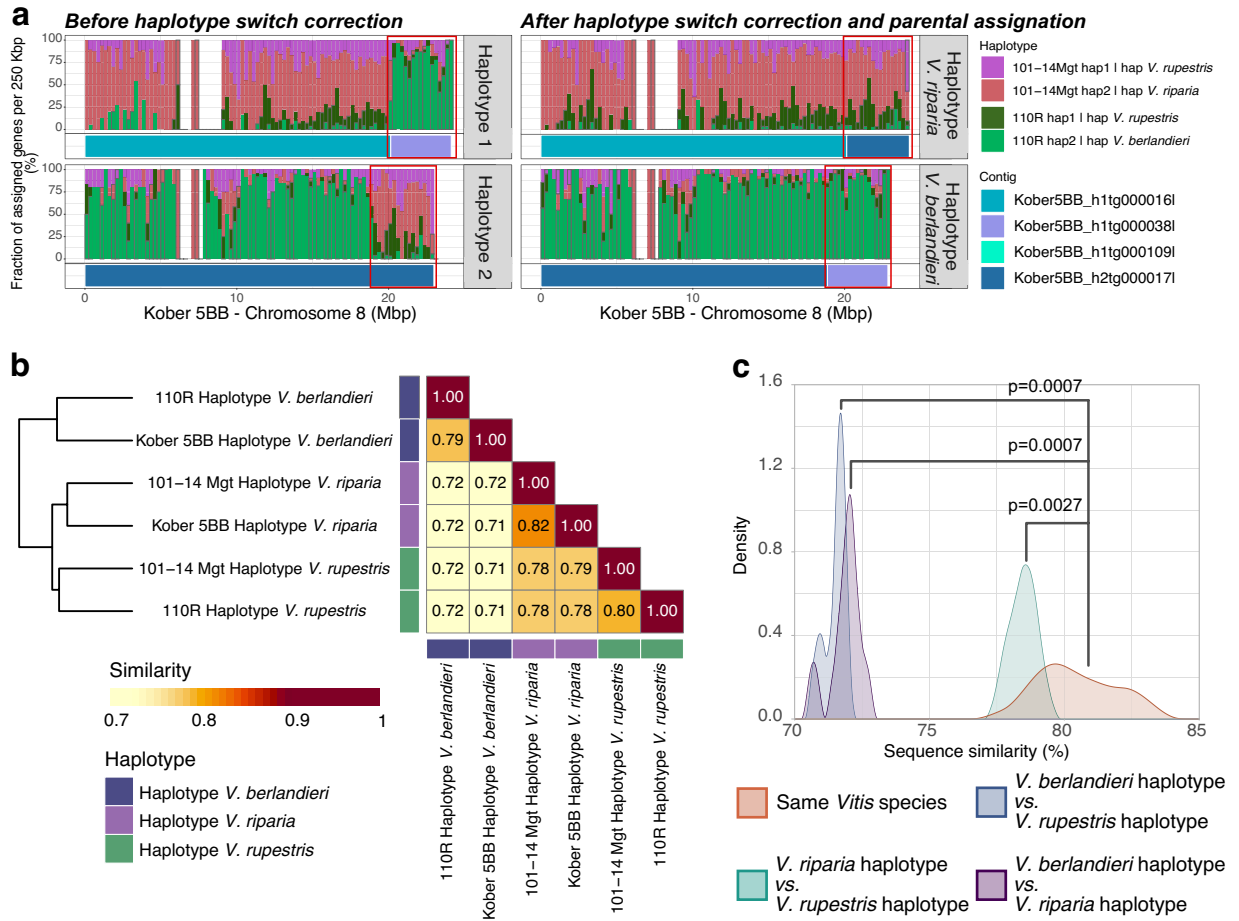


Fig. 3 Haplotyping based on intraspecific sequence similarity. Shared parental species information was used to assign each haplotype to either *V. riparia*, *V. rupestris*, or *V. berlandieri* based on sequence similarity. This allowed to resolved assembly errors (i.e. haplotype switches). **(a)** Example of an haplotype switch found on chromosome 8 of Kober 5BB (left panel). After scaffolding of the pseudomolecules, an haplotype switch was observed at the end of chromosome 8 of Kober 5BB. The genes in the contig Kober5BB_h1tg000016l on haplotype 1 were highly similar to the genes located in 101–14 Mgt haplotype 2 (red), suggesting that Kober5BB_h1tg000016l derived from *V. riparia*, whereas the genes of Kober5BB_h1tg000038l corresponded to genes in haplotype 2 of chromosome 8 of 110R (light green), suggesting that Kober5BB_h1tg000038l derived from *V. berlandieri*. An opposite pattern was observed on haplotype 2, with the genes of the first 18.9 Mbp of the pseudomolecule similar to the genes of the haplotype 2 of 110R (light green) and the genes from the last 4.2 Mbp similar to the genes of the haplotype 2 of 101–14 Mgt haplotype 2 (red). The haplotype switch was corrected by interchanging the contig Kober5BB_h1tg000038l with the corresponding region in the alternative haplotype, consisting of Kober5BB_h2tg000109l and 4.2 Mbp of Kober5BB_h2tg000017l (right panel). **(b)** Sequence similarity between haplotypes represented as the average percentage of the haploid chromosome set length not affected by structural variants (>50 bp), SNPs or InDels when compared with another haplotype. **(c)** Distribution of the percentage of sequence similarity (as defined in B) between haplotypes derived from the same species and haplotypes derived from different species (Statistical testing was performed with pairwise Wilcoxon rank sum test, density plot was produced with adjust = 1, n = 4096, kernel = “cosine” parameters).

GeneMark v.3.47³³, and SNAP v.2006-07-28³⁴. For the repeat annotation, RepeatMasker v.open-4.0.6³⁵ was used. To assign a functional annotation to each of these gene models, results from diamond v2.0.13.151^{36,37} blastp matches on the Refseq plant protein database (<https://ftp.ncbi.nlm.nih.gov/refseq/>, retrieved January 17th, 2019) and from InterProScan v.5.28–67.0³⁸ were parsed through Blast2GO v.4.1.9³⁹. A total of 56,768 protein-coding gene loci were annotated in the genome assembly of 110R, 59,807 in Kober 5BB and 72,758 in 101–14 Mgt. On average, 124,991 ± 36,197 protein-coding alternative splicing variants were identified per haplotype. The unplaced sequences were composed of 2,747 ± 2,821 gene loci (Table 1).

Analysis of colinearity between haplotypes. Colinear gene loci were identified using MCScanX v.11. Nov.2013⁴⁰. Annotated protein-coding sequences of the three rootstocks were aligned against each other using GMAP v.2019-09-12⁴¹ with the parameters “-B 4 -x 30-split-output”. Alignments with both identity and coverage

greater than 80% were retained. Alignments corresponding to annotated mRNA regions were identified using mapBed from Bedtools v2.29.2⁴² with the parameters “-F 0.75 -f 0.5 -e”. Colinear blocks were then detected with MCScanx_h (MCScanX v.11.Nov.2013⁴⁰) tool using the following parameters “-s 10 -m 5 -w 5”.

Identification of sequence polymorphisms and structural variants between haplotypes. Pseudomolecule sequences were aligned against each other using nucmer tool from MUMmer4 v.4.0.0.beta5⁴³. SNPs and short indels between haplotypes were identified from alignments with show-snps tool (MUMmer4 v.4.0.0.beta5⁴³) with parameters “-Clr -x” and longer structural variants with show-diff tool (MUMmer4 v.4.0.0.beta5⁴³) with default parameters.

Data Records

Sequencing data were deposited at NCBI under BioProject number PRJNA858084, SRA accessions SRR20810421⁴⁴, SRR20810422⁴⁵, SRR20810423⁴⁶, SRR20810424⁴⁷, SRR20810425⁴⁸, SRR20810426⁴⁹, and SRR20810427⁵⁰. Genome assemblies are available at EMBL-EBI under BioProject number PRJEB55013⁵¹. Genome assemblies, gene annotation and repeat annotation files are at Zenodo under the <https://doi.org/10.5281/zenodo.6824323>⁵², and at <http://www.grapegenomics.com>⁵³. A genome browser and a blast tool are available for each rootstock at <http://www.grapegenomics.com>⁵³.

Technical Validation

The genome assemblies were evaluated for completeness of the diploid sequence and gene content, and for correct haplotype phasing. The average size of each set of 19 pseudomolecules was 494.5 ± 5.5 Mbp (diploid genome size: $1,015.0 \pm 7.9$ Mbp, Supplemental figure 1), which is close to the length of the parental haploid genome size estimated by flow cytometry (499.3 ± 37.3 Mbp⁵⁴) suggesting that the three genomes were entirely assembled. Only 36.1 Mbp (3.5%), 19.9 Mbp (2.0%), and 23.3 Mbp (2.3%) of the draft sequences could not be placed into any pseudomolecules of 101–14 Mgt, 110R, and Kober 5BB genomes, respectively. The unplaced sequences were mostly composed of repeats ($68.0\% \pm 12.3\%$). These results are comparable with the latest release of the *V. vinifera* PN40024 reference haploid genome assembly, for which the location of 27.4 Mbp (5.6%) remains undetermined⁵⁵.

Each set of 19 pseudomolecules was evaluated for gene space completeness using both conserved single-copy orthologs of plant genes (BUSCOs) and the single-copy gene content of *V. vinifera* PN40024. Complete copies of $98.1 \pm 0.14\%$ of the BUSCO models were found in each set of pseudomolecules (Supplemental Table 1). Similarly, almost all of the single-copy genes of PN40024 aligned to each set of pseudomolecules ($95.01\% \pm 0.3\%$). The gene space present in the unplaced sequences was limited to $0.69 \pm 0.8\%$ of the BUSCO models and $1.79 \pm 0.8\%$ of the PN40024 genes. The completeness of the gene space is another strong evidence that the assemblies are a complete representation of the diploid genomes of the three rootstocks. On both haplotypes of 101–14 Mgt we found more gene loci ($33,379 \pm 328$) than in 110R and Kober 5BB ($28,584 \pm 863$). Further genome-wide gene expression analyses are required to determine if the larger number of gene loci identified in 101–14 Mgt corresponds to a larger number of expressed transcripts than in the other rootstocks.

Using the pedigree information of each rootstock (Fig. 1b), we assigned each pseudomolecule to its parental *Vitis* species, i.e. either *V. riparia*, *V. rupestris*, or *V. berlandieri*. For each pseudomolecule, we identified the three pairs of haplotypes having the highest gene sequence similarity and assigned them to the shared parental *Vitis* species. This allowed us to manually detect and correct the phasing errors (i.e. haplotype switches) introduced during the assembly of the draft sequences or the scaffolding of the pseudomolecules (Fig. 3a). Whole-sequence comparison of the six haplotypes of each pseudomolecule showed that the haplotypes assigned to the same *Vitis* species were more similar ($80.5\% \pm 1.4\%$ identity) than those that do not share the same species ($74.0\% \pm 3.3\%$ identity; p value = 0.0003, $W = 142$, $n = 30$ unpaired Wilcoxon rank sum test; Fig. 3b,c). These results suggest that the haplotypes of the three rootstock genomes were correctly phased. Despite the variable levels of sequence polymorphism, pseudomolecules of the three rootstock genomes were highly colinear regardless of their species of origin. When considering both gene sequence similarity, gene order, and physical location, $73.1\% \pm 3.5\%$ of the protein-coding loci were found in at least one colinear block when comparing haplotypes with shared parental origin, and $71.5\% \pm 3.5\%$ between haplotypes of different species (Supplemental figure 2). Overall, an average of $82.4\% \pm 2.6\%$ of the genomic sequences are covered by colinear blocks (Supplemental figure 3), which reflects a remarkable conservation of chromosome structure among these *Vitis* species.

Code availability

The pipeline used for gene structural and functional annotation is available in details at https://github.com/andreaminio/AnnotationPipeline-EVM_based-DClab.

Received: 4 August 2022; Accepted: 30 September 2022;

Published online: 28 October 2022

References

1. Millardet, A. *Histoire des principales variétés et espèces de vignes d'origine américaine qui résistent au phylloxera* (G. Masson, Paris, 1885).
2. Dodson Peterson, J. C. *et al.* Grape Rootstock Breeding and Their Performance Based on the Wolpert Trials in California. In Cantu, D. & Walker, M. A. (eds.) *The Grape Genome*, 301–318, https://doi.org/10.1007/978-3-030-18601-2_14 (Springer International Publishing, Cham, 2019).
3. Pongracz, D. P. Rootstocks for grape-vines. Publisher: Cape Town (South Africa) David Philip (1983).
4. Ravaz, L. *Les vignes américaines: porte-greffes et producteurs-directs: caractères, aptitudes* (Goulet, 1902).

5. Riaz, S. *et al.* Genetic diversity and parentage analysis of grape rootstocks. *Theoretical and Applied Genetics* **132**, 1847–1860, <https://doi.org/10.1007/s00122-019-03320-5> (2019).
6. Christensen, L. P. Rootstock selection. *Wine grape varieties in California*. University of California, Oakland, CA, USA 12–15 (2003).
7. Dodson Peterson, J. C. & Andrew Walker, M. Influence of Grapevine Rootstock on Scion Development and Initiation of Senescence. *Catalyst: Discovery into Practice* **1**, 48, <https://doi.org/10.5344/catalyst.2017.16006> (2017).
8. Ferris, H., Zheng, L. & Walker, M. A. Resistance of Grape Rootstocks to Plant-parasitic Nematodes. *Journal of nematology* **44**, 377–386 (2012).
9. Rahemi, A., Dodson Peterson, J. C. & Lund, K. T. *Grape Rootstocks and Related Species* (Springer International Publishing, Cham, 2022).
10. Girollet, N. *et al.* De novo phased assembly of the *Vitis riparia* grape genome. *Scientific Data* **6**, 1–8, 10/ghdrm3 (2019).
11. Patel, S. *et al.* Draft genome of the Native American cold hardy grapevine *Vitis riparia* Michx. ‘Manitoba 37’. *Horticulture Research* **7**, 10/gg53d4. ISBN: 4143802003162 Publisher: Springer US (2020).
12. Cheng, H., Concepcion, G. T., Feng, X., Zhang, H. & Li, H. Haplotype-resolved de novo assembly using phased assembly graphs with hifiasm. *Nature Methods* **18**, 170–175, 10/ghz4s5 (2021).
13. Minio, A., Cochetel, N., Vondras, A. M., Massonnet, M. & Cantu, D. Assembly of complete diploid-phased chromosomes from draft genome sequences. *G3 Genes|Genomes|Genetics* **jkac143**, <https://doi.org/10.1093/g3journal/jkac143> (2022).
14. Chin, C. S. *et al.* Phased diploid genome assembly with single-molecule real-time sequencing. *Nature Methods* **13**, 1050–1054 (2016). 10/f9fv4w.
15. Blanco-Ulate, B., Vincenti, E., Powell, A. L. & Cantu, D. Tomato transcriptome and mutant analyses suggest a role for plant stress hormones in the interaction between fruit and *Botrytis cinerea*. *Frontiers in Plant Science* **4**, 1–16, 10/gkzgz3v (2013).
16. Manni, M., Berkeley, M. R., Seppy, M., Simão, F. A. & Zdobnov, E. M. BUSCO Update: Novel and Streamlined Workflows along with Broader and Deeper Phylogenetic Coverage for Scoring of Eukaryotic, Prokaryotic, and Viral Genomes. *Molecular Biology and Evolution* **38**, 4647–4654, <https://doi.org/10.1093/molbev/msab199> (2021).
17. Jaillon, O. *et al.* The grapevine genome sequence suggests ancestral hexaploidization in major angiosperm phyla. *Nature* **449**, 463–467, 10/ckfnh2 (2007).
18. Zou, C. *et al.* Haplotyping the *Vitis* collinear core genome with rhAmpSeq improves marker transferability in a diverse genus. *Nature Communications* **11**, 413, 10/ghdrnk. Publisher: Springer US (2020).
19. Massonnet, M. *et al.* The genetic basis of sex determination in grapes. *Nature communications* **11**, 2902, 10/gjxrfm. Publisher: Springer US (2020).
20. Li, H. Minimap2: Pairwise alignment for nucleotide sequences. *Bioinformatics* **34**, 3094–3100, 10/gdhhqt. [eprint: 1708.01492](https://doi.org/10.1093/bioinformatics/bty183) (2018).
21. Cochetel, N. *et al.* Diploid chromosome-scale assembly of the *Muscadinia rotundifolia* genome supports chromosome fusion and disease resistance gene expansion during *Vitis* and *Muscadinia* divergence. *G3 Genes|Genomes|Genetics* **11**, jkab033, <https://doi.org/10.1093/g3journal/jkab033> (2021).
22. Au, K. F., Underwood, J. G., Lee, L. & Wong, W. H. Improving PacBio Long Read Accuracy by Short Read Alignment. *PLoS ONE* **7**, 1–8, 10/f383xz (2012).
23. Bolger, A. M., Lohse, M. & Usadel, B. Trimmomatic: A flexible trimmer for Illumina sequence data. *Bioinformatics* **30**, 2114–2120, 10/f6cj5w (2014).
24. Haas, B. J. *et al.* De novo transcript sequence reconstruction from RNA-seq using the Trinity platform for reference generation and analysis. *Nature Protocols* **8**, 1494–1512, 10/f22qdv (2013).
25. Pertea, M. *et al.* StringTie enables improved reconstruction of a transcriptome from RNA-seq reads. *Nature Biotechnology* **33**, 290–295, 10/f64s85 (2015).
26. Kim, D., Langmead, B. & Salzberg, S. L. HISAT: A fast spliced aligner with low memory requirements. *Nature Methods* **12**, 357–360 (2015). 10/f67q59.
27. Li, W. & Godzik, A. Cd-hit: A fast program for clustering and comparing large sets of protein or nucleotide sequences. *Bioinformatics* **22**, 1658–1659, 10/ct8g72 (2006).
28. Haas, B. J. *et al.* Improving the Arabidopsis genome annotation using maximal transcript alignment assemblies. *Nucleic Acids Research* **31**, 5654–5666, 10/cgkkwd (2003).
29. Slater, G. S. C. & Birney, E. Automated generation of heuristics for biological sequence comparison. *BMC Bioinformatics* **6**, 1–11, <https://doi.org/10.1186/1471-2105-6-31> (2005).
30. Haas, B. J. *et al.* Automated eukaryotic gene structure annotation using EVidenceModeler and the Program to Assemble Spliced Alignments. *Genome Biology* **9**, <https://doi.org/10.1186/gb-2008-9-1-r7> (2008).
31. Stanke, M., Tzvetkova, A. & Morgenstern, B. AUGUSTUS at EGASP: using EST, protein and genomic alignments for improved gene prediction in the human genome. *Genome biology* **7**(Suppl 1), 1–8, <https://doi.org/10.1186/gb-2006-7-s1-s11> (2006).
32. Seppy, M., Manni, M. & Zdobnov, E. M. *Gene Prediction: Methods and Protocols*, vol. 1962 of *Methods in Molecular Biology* (Springer New York, New York, NY, 2019).
33. Lomsadze, A., Ter-Hovhannisyanyan, V., Chernoff, Y. O. & Borodovsky, M. Gene identification in novel eukaryotic genomes by self-training algorithm. *Nucleic Acids Research* **33**, 6494–6506 (2005). 10/bz9c2v.
34. Korf, I. Gene finding in novel genomes. *BMC Bioinformatics* **5**, 59, 10/cdvb5x. ISBN: 1471-2105 (Electronic) (2004).
35. Smit, A. F. A., Hubley, R. & Green, P. RepeatMasker Open-4.0. Pages: 2013–2015 Publication Title: <http://www.repeatmasker.org> (2013).
36. Buchfink, B., Xie, C. & Huson, D. H. Fast and sensitive protein alignment using DIAMOND. *Nature Methods* **12**, 59–60, <https://doi.org/10.1038/nmeth.3176> (2015).
37. Buchfink, B., Reuter, K. & Drost, H.-G. Sensitive protein alignments at tree-of-life scale using DIAMOND. *Nature Methods* **18**, 366–368, <https://doi.org/10.1038/s41592-021-01101-x> (2021).
38. Jones, P. *et al.* InterProScan 5: genome-scale protein function classification. *Bioinformatics (Oxford, England)* **30**, 1236–40, 10/f53532 (2014).
39. Conesa, A. *et al.* Blast2GO: A universal tool for annotation, visualization and analysis in functional genomics research. *Bioinformatics* **21**, 3674–3676, <https://doi.org/10.1093/bioinformatics/bti610> (2005).
40. Wang, Y. *et al.* MCScanX: A toolkit for detection and evolutionary analysis of gene synteny and collinearity. *Nucleic Acids Research* **40**, 1–14, 10/fzn3xm (2012).
41. Wu, T. D. & Watanabe, C. K. GMAP: A genomic mapping and alignment program for mRNA and EST sequences. *Bioinformatics* **21**, 1859–1875, 10/cjb8q8 (2005).
42. Quinlan, A. R. & Hall, I. M. BEDTools: A flexible suite of utilities for comparing genomic features. *Bioinformatics* **26**, 841–842, <https://doi.org/10.1093/bioinformatics/btq033> (2010).
43. Marçais, G. *et al.* MUMmer4: A fast and versatile genome alignment system. *PLoS Computational Biology* **14**, e1005944, 10/gcw64s (2018).
44. NCBI Sequence Read Archive <https://identifiers.org/ncbi/insdc.sra:SRR20810421> (2022).
45. NCBI Sequence Read Archive <https://identifiers.org/ncbi/insdc.sra:SRR20810422> (2022).
46. NCBI Sequence Read Archive <https://identifiers.org/ncbi/insdc.sra:SRR20810423> (2022).
47. NCBI Sequence Read Archive <https://identifiers.org/ncbi/insdc.sra:SRR20810424> (2022).

48. NCBI Sequence Read Archive <https://identifiers.org/ncbi/insdc.sra:SRR20810425> (2022).
49. NCBI Sequence Read Archive <https://identifiers.org/ncbi/insdc.sra:SRR20810426> (2022).
50. NCBI Sequence Read Archive <https://identifiers.org/ncbi/insdc.sra:SRR20810427> (2022).
51. ENA European Nucleotide Archive, <https://identifiers.org/ena.embl:PRJEB55013> (2022).
52. Minio, A., Cantu, D., Cochetel, N., Massonnet, M. & Figueroa-Balderas, R. Supporting data: HiFi chromosome-scale diploid assemblies of the grape rootstocks 110R, Kober 5BB, and 101–14 Mgt. *Zenodo* <https://doi.org/10.5281/zenodo.6824323> (2022).
53. Minio, A. & Cantu, D. Grapegenomics.com: a web portal with genomic data and analysis tools for wild and cultivated grapevines. *Zenodo* <https://doi.org/10.5281/zenodo.7027886> (2022).
54. Lodhi, M. A. & Reisch, B. I. Nuclear DNA content of Vitis species, cultivars, and other genera of the Vitaceae. *Theoretical and Applied Genetics* **90**, 11–16, 10/cgwkss (1995).
55. Canaguier, A. *et al.* A new version of the grapevine reference genome assembly (12X.v2) and of its annotation (VCost.v3). *Genomics Data* **14**, 56–62, <https://doi.org/10.1016/j.gdata.2017.09.002> (2017).

Acknowledgements

The RNAseq data of *V. rupestris* were kindly provided by Dr. Jason Londo, Cornell University. This work was funded by the NSF grant #1741627 and partially supported by funds to D.C. from the Louis P. Martini Endowment in Viticulture.

Author contributions

A.M., N.C. and D.C. conceived the work. A.M. conducted the bioinformatic analyses. R.F.-B. performed all the wet-lab activities associated with the project. A.M., N.C., M.M., D.C. wrote the manuscript.

Competing interests

The authors declare no competing interests.

Additional information

Supplementary information The online version contains supplementary material available at <https://doi.org/10.1038/s41597-022-01753-0>.

Correspondence and requests for materials should be addressed to D.C.

Reprints and permissions information is available at www.nature.com/reprints.

Publisher's note Springer Nature remains neutral with regard to jurisdictional claims in published maps and institutional affiliations.



Open Access This article is licensed under a Creative Commons Attribution 4.0 International License, which permits use, sharing, adaptation, distribution and reproduction in any medium or format, as long as you give appropriate credit to the original author(s) and the source, provide a link to the Creative Commons license, and indicate if changes were made. The images or other third party material in this article are included in the article's Creative Commons license, unless indicated otherwise in a credit line to the material. If material is not included in the article's Creative Commons license and your intended use is not permitted by statutory regulation or exceeds the permitted use, you will need to obtain permission directly from the copyright holder. To view a copy of this license, visit <http://creativecommons.org/licenses/by/4.0/>.

© The Author(s) 2022